Alexandria Engineering Journal (2015) 54, 35–44

HOSTED BY
ELSEVIER

Alexandria University
Alexandria Engineering Journal
www.elsevier.com/locate/aej
www.sciencedirect.com

ORIGINAL ARTICLE

Thermophoretic MHD slip flow over a permeable surface with variable fluid properties

K. Das [a], **S. Jana** [b,*], **P.K. Kundu** [b]

[a] Dept. of Mathematics, Kalyani Govt. Engg. College, Kalyani 741235, West Bengal, India
[b] Dept. of Mathematics, Jadavpur University, Kolkata 700032, West Bengal, India

Received 6 January 2014; revised 29 July 2014; accepted 23 November 2014
Available online 20 December 2014

KEYWORDS

Thermophoresis;
Slip fow;
Variable viscosity;
Variable thermal conductivity;
MHD;
Permeable surface

Abstract The present paper focuses on the analysis of thermophoretic hydromagnetic slip flow over a permeable flat plate with convective surface heat flux at the boundary and temperature dependent fluid properties in the presence of non-uniform heat source/sink. The transverse magnetic field is assumed to be a function of the distance from the origin. Also it is assumed that the liquid viscosity and the thermal conductivity vary as an inverse function and a linear function of temperature, respectively. The shooting method is employed to yield the numerical solutions for the model. Results show that the thermal boundary layer thickness reduces with increase of surface convection parameter whereas reverse effect occurs for viscosity parameter. It is also observed that the thermophoretic parameter decreases the concentration distribution across the boundary layer.

1. Introduction

Recently, research on aerosol particles deposition has become more and more important for engineering applications. The factors that influence particle deposition include convection, inertial impaction, sedimentation, Brownian diffusion, thermophoresis, electrophoresis, etc. Thermophoresis is an important mechanism of micro-particle transport due to a temperature gradient in the surrounding medium and has found numerous applications, especially in the field of aerosol technology. When a temperature gradient exists in the field surrounding a small particle, a net force is exerted on the particle due to an imbalance of the forces associated with molecular collisions from the hotter and colder region. Due to thermophoresis, small micron sized particles are deposited on cold surfaces. In this process, the repulsion of particles from hot objects also takes place and a particle-free layer is observed around hot bodies (see Goldsmith and May [1]). This phenomenon has many practical applications in removing small particles from gas particle trajectories, from combustion devices, and studying the particulate material deposition turbine blades. Thermophoretic deposition of radioactive particles is considered to be one of the important factors causing accidents in nuclear reactors. Many studies were reported considering the effect of thermophoresis on the boundary layer [2–8]. Partha [9] investigated suction/injection effects on thermophoresis particle deposition in a non-Darcy porous medium. The effects of thermophoresis and radiation on laminar flow were studied

* Corresponding author.
E-mail addresses: kd_kgec@rediffmail.com (K. Das), jana05subrata@gmail.com (S. Jana), kunduprabir@yahoo.co.in (P.K. Kundu).
Peer review under responsibility of Faculty of Engineering, Alexandria University.

http://dx.doi.org/10.1016/j.aej.2014.11.005
1110-0168

by Bakier and Gorla [10]. A recent paper by Postelnicu [11] dealt with the effects of thermophoretic particle deposition on the natural convection flow over an inclined porous media.

The magnetohydrodynamic (MHD) boundary layer flow for an electrically conducting fluid in porous medium is of considerable interest in geothermal engineering, energy conservation, modern metallurgical processes, underground disposal of nuclear waste materials and many others. Thermophoresis is also a key mechanism of study in semi-conductor technology especially controlled high quality wafer production as well as MHD energy generation system operations. Since various industrial heat transfer processes involved both the hydromagnetic flows and thermophoresis such as in MHD energy systems, many numerical studies [12–15] on magnetohydrodynamic heat and mass transfer have been reported with buoyancy, Joule heating effects and heat source/sink parameters. Recently, the effects of thermophoresis and internal heat generation/absorption on MHD heat and mass transfer flow over an inclined radiate permeable surface were examined by Noor et al. [16]. All of these studies, however, considered constant fluid properties and no-slip at the boundary. In certain situations, the assumption of no-slip boundary condition does no longer apply. When fluid flows in micro electro mechanical system (MEMS), the no slip condition at the solid-fluid interface is no longer applicable. Slip flow happens if the characteristic size of the flow system is small or the flow pressure is very low. A partial slip may occur on a stationary and moving boundary when the fluid is particulate such as emulsions, suspensions, foams, and polymer solutions. On the other hand most of the MHD applications in microfluidics are in the liquid fields. Thus considering MHD liquid slip flow has promising potential in numerous practical applications such as MHD micro pumps which are a non-mechanical pump. The slip flows under different flow configurations have been studied in recent years [17–21]. Recently, Das [22] have considered the slip effects on heat and mass transfer in MHD micropolar fluid flow over an inclined plate with thermal radiation and chemical reaction.

All of these studies, however, considered constant thermophysical properties such as constant viscosity and thermal conductivity. But, it is well known [23–28] that these physical properties may change with temperature, especially fluid viscosity, thermal conductivity, etc. For lubricating fluids, heat generated by internal friction and the corresponding rise in the temperature affects the physical properties of the fluid and so the properties of the fluid are no longer assumed to be constant. The increase in temperature leads to increase in the transport phenomena by reducing the physical properties across the thermal boundary layer and so the heat transfer at the wall is also affected. Therefore to predict the flow and heat transfer rates, it is necessary to take into account the variable fluid properties. Zueco et al. [29] discussed the effect of thermophoresis particle deposition and of the thermal conductivity in a porous plate with dissipative heat and mass transfer. Recently, Das [30] investigated the impact of thermal radiation on MHD slip flow over a flat plate with variable fluid properties.

To our best knowledge, study on MHD heat and mass transfer slip flow over a radiate permeable surface with thermophoretic particle deposition and variable liquid properties has never been considered till date. Therefore, in this paper, the previous work of Das [30] is extended to include the thermophoretic parameters for both suction and injection. The present objective is to investigate the effects of variable fluid properties with thermophoretic particle deposition for both suction and injection cases.

2. Formulation of the problem

2.1. Governing equations and boundary conditions

Consider a two dimensional steady laminar flow of an incompressible electrically conducting liquid over a radiating permeable flat plate in the presence of a transverse magnetic field $\vec{B}$ (see Fig. 1). The magnetic Reynolds number of the flow is taken to be small enough so that induced magnetic field is assumed to be negligible in comparison with applied magnetic field. Thus $\vec{B} = [0, B(x)]$, where $B(x)$ is the applied magnetic field acting normal to the plate and varies in strength as a function of x. The flow is assumed to be in the x-direction which is taken along the plate and y-axis is normal to it. Suction or injection is imposed on the permeable plate. The viscosity and thermal conductivity of the liquid are assumed to be functions of temperature. The presence of non-uniform heat source/sink and thermophoresis is considered to study the variation of heat transfer and concentration deposition on the flat surface. The pressure gradient, body forces, viscous dissipation and Joule heating effects are neglected in comparison with the effect of heat source/sink. The temperature of the plate surface is held uniform at T_w which is higher than the ambient temperature T_∞. The species concentration at the surface is maintained uniform at C_w while the ambient liquid concentration is assumed to be C_∞.

Under the boundary layer approximations, the conservation equations for the flow regime can be shown to take the following form: (see Ref. [27,30])

$$\frac{\partial u}{\partial x} + \frac{\partial v}{\partial y} = 0, \tag{1}$$

$$\rho\left(u\frac{\partial u}{\partial x} + v\frac{\partial u}{\partial y}\right) = \frac{\partial}{\partial y}\left(\mu\frac{\partial u}{\partial y}\right) - \sigma B^2(x)(u - U_\infty), \tag{2}$$

$$\rho c_p\left(u\frac{\partial T}{\partial x} + v\frac{\partial T}{\partial y}\right) = \frac{\partial}{\partial y}\left[\left(\kappa + \frac{16T_\infty^3\sigma^*}{3k^*}\right)\frac{\partial T}{\partial y}\right] + q''', \tag{3}$$

$$u\frac{\partial C}{\partial x} + v\frac{\partial C}{\partial y} = D\frac{\partial^2 C}{\partial y^2} - \frac{\partial(V_T C)}{\partial y}, \tag{4}$$

where u, v are velocity components along x, y-axis respectively, U_∞ is the free stream velocity, σ is the electrical conductivity of the liquid, T is the temperature of the liquid within the boundary layer, κ is the thermal conductivity of the liquid, c_p is the specific heat at constant pressure p, μ is the dynamic viscosity, ρ is the constant liquid density, σ^* is the Stefan–Boltzmann constant and k^* is the mean absorption coefficient, C is the concentration of the liquid within the boundary layer and D is the molecular diffusivity of the species concentration. The thermophoretic velocity V_T can be written as (see Ref. Talbot et al. [3])

$$V_T = kv\frac{\nabla T}{T_r} = -\frac{kv}{T_r}\frac{\partial T}{\partial y} \tag{5}$$

where T_r is a reference temperature and k is the thermophoretic coefficient which ranges in value from 0.2 to 1.2 as indicated by Batchelor and Shen [4] and is defined from the theory of Talbot et al. [3] by

$$k = \frac{2C_s(\lambda_g/\lambda_p + C_t Kn)[C_1 + C_2 e^{-C_3/Kn}]}{(1 + 3C_m Kn)(1 + 2\lambda_g/\lambda_p + 2C_t Kn)} \tag{6}$$

where $C_1,\ C_2,\ C_3,\ C_m,\ C_s,\ C_t$ are constant, λ_g and λ_p are the thermal conductivities of the liquid and diffused particles, respectively, and Kn is the Knudsen number. The thermophoretic parameter τ can be defined as (see Ref. Goren [2])

$$\tau = -\frac{k(T_w - T_\infty)}{T_r} \tag{7}$$

Typical values of τ are 0.01, 0.05 and 0.1 corresponding to approximate values of $-k(T_w - T_\infty)$ equal to 3 K, 15 K and 30 K for a reference temperature of $T_r = 300$ K.

The liquid viscosity is assumed to be an inverse linear function of temperature given by the following (see Ref. Ling and Dybbs [31])

$$\frac{1}{\mu} = \frac{1}{\mu_\infty}[1 + \chi(T - T_\infty)] \tag{8}$$

where μ_∞ is the dynamic viscosity at ambient temperature and χ is the thermal property of liquid.

Eq. (8) can be written as follows:

$$\frac{1}{\mu} = a(T - T_r) \tag{9}$$

where $a = \frac{\chi}{\mu_\infty}$ and $T_r = T_\infty - \frac{1}{\chi}$ are constant and their values depend on the reference state and the thermal property of the liquid. Following Chiam [23] and Savvas et al. [33], we consider the specific model for variable thermal conductivity as

$$\kappa = \kappa_\infty\left(1 + \epsilon\frac{T - T_\infty}{\Delta T}\right) \tag{10}$$

where κ_∞ is the thermal conductivity at ambient temperature, $\Delta T = T_w - T_\infty$ and ϵ is a thermophysical constant dependent on the liquid ($\epsilon < 0$ for lubrication oils, hydromagnetic working liquids and $\epsilon > 0$ for water)

The non-uniform heat source/sink q''' is given by (see Ref. Das [30], Abo-Eldahab and EI-Aziz [32])

$$q''' = \frac{\kappa_\infty U_0}{2v_\infty x}[Q(T - T_\infty) + Q^*(T_w - T_\infty)e^{-\beta' y}] \tag{11}$$

where Q and Q^* are the coefficients of space and temperature dependent heat source/sink terms respectively and β' is the thermal property of liquid. The case $Q > 0,\ Q^* > 0$ corresponds to internal heat generation while $Q < 0,\ Q^* < 0$ corresponds to internal heat absorption.

The appropriate boundary conditions for the present problem are

$$\left.\begin{array}{l} \left.\begin{array}{l} u = u_s(slip\ velocity), v = -V_0(x)(permeable\ surface), C = C_w \\ -\kappa\frac{\partial T}{\partial y} = h_w(T_w - T)(convective\ surface\ heat\ flux) \end{array}\right\} for\ y = 0, \\ u = U_\infty, T = T_\infty, C = C_\infty as\ y \to \infty \end{array}\right\} \tag{12}$$

where V_0 is the transpiration velocity at the wall. For mass injection into the boundary layer (blowing), $V_0 < 0$; for mass removal from the boundary layer (suction), $V_0 > 0$. h_w is the convective heat transfer coefficient and u_s is the slip velocity which is assumed to be proportional to the local wall shear stress as follows:

$$u_s = l\frac{\partial u}{\partial y}|_{y=0} \tag{13}$$

where l is slip length as a proportional constant of the velocity slip. To obtain solutions in the slip-flow domain, liquid velocity and thermal conditions must be specified at the boundaries. In liquids, however, the molecules are densely packed and a mean free path is not a meaningful quantity. For liquids, therefore, l is defined as the inter action length. It is to be mentioned that temperature jump condition due to slip flow is neglected in the present study.

2.2. Similarity transformation

Let us introduce the following dimensionless variables which will convert the partial differential equations from two independent variables (x, y) to a system of coupled, non-linear ordinary differential equations in a single variable (η):

$$\eta = y\sqrt{\frac{U_\infty}{v_\infty x}},\ \psi = \sqrt{(U_\infty v_\infty x)}f(\eta),$$
$$\theta(\eta) = \frac{T - T_\infty}{T_w - T_\infty},\ \phi(\eta) = \frac{C - C_\infty}{C_w - C_\infty} \tag{14}$$

where $\psi(x, y)$ is the stream function that satisfies the continuity Eq. (1) with

$$u = \frac{\partial\psi}{\partial y} = U_\infty f' \quad and \quad v = -\frac{\partial\psi}{\partial x} = -\frac{1}{2}\sqrt{\frac{v_\infty U_\infty}{x}}(f - \eta f') \tag{15}$$

where f is non-dimensional stream function and prime denotes differentiation with respect to η and $v_\infty = \mu_\infty/\rho$ is the kinematic viscosity of the ambient liquid.

The dimensionless temperature θ can also be written as

$$\theta = \frac{T - T_r}{T_w - T_\infty} + \theta_r \tag{16}$$

where $\theta_r = T_r - T_\infty/(T_w - T_\infty) = -1/\delta(T_w - T_\infty)$ and its value is determined by the viscosity/temperature characteristics of the liquid under consideration and the operating temperature difference. If θ_r is large i.e., if $T_w - T_\infty$ is small, the effects of variable viscosity on the flow can be neglected. On the other hand, for smaller values of θ_r, either the liquid viscosity changes markedly with temperature or the operating temperature difference is high. It is important to note that θ_r is negative for liquids.

Using (16), Eq. (9) becomes

$$\mu = \mu_\infty\left(\frac{\theta_r}{\theta_r - \theta}\right) \tag{17}$$

This viscosity model is very much appropriate for the present study than other models such as the Reynolds and Vogel's viscosity models because it is valid for wider range of temperatures.

The relation (10) can also be written as

$$\kappa = \kappa_\infty(1+\epsilon\theta) \tag{18}$$

where ϵ is the thermal conductivity variation parameter.

The equations of motion are thereby reduced from Eqs. (2)–(4) to the following dimensionless similarity form:

$$\left(\frac{\theta_r}{\theta_r-\theta}\right)f''' + \frac{1}{2}ff'' + \frac{\theta_r}{(\theta_r-\theta)^2}f''\theta' - M^2(f'-1) = 0, \tag{19}$$

$$(1+\epsilon\theta+Nr)\theta'' + \epsilon\theta'^2 + \frac{1}{2}Pr_\infty f\theta' + Q\theta + Q^* e^{-\beta\eta} = 0, \tag{20}$$

$$\phi'' + Sc(f-\tau\theta')\phi' - Sc\tau\theta''\phi = 0, \tag{21}$$

where $M = B(x)\sqrt{\frac{\sigma x}{\rho U_\infty}}$ is the magnetic field parameter, $Pr_\infty = \mu_\infty c_p/\kappa_\infty$ is the ambient Prandtl number, $Nr = 16T_\infty^3\sigma^*/3k^*\kappa_\infty$ is the thermal radiation parameter, $\beta = \beta'\sqrt{\frac{v_\infty x}{U_\infty}}$ is the thermal property of fluid and $Sc = v/D_m$ is the Schmidt number.

The corresponding boundary conditions (12) become

$$\left.\begin{array}{l} f = f_w, f' = \delta f'', \theta' = -\zeta\left(\frac{1-\theta(0)}{1+\epsilon\theta(0)}\right), \phi = 1 \; for \; \eta = 0, \\ f' = 1, \theta = 0, \phi = 0 \; as \; \eta \to \infty \end{array}\right\} \tag{22}$$

where $\zeta = \frac{h_w}{\kappa_\infty}\sqrt{\frac{v_\infty x}{U_\infty}}$ is the surface convection parameter, $\delta = L\sqrt{\frac{U_\infty}{v_\infty x}}$ is the slip parameter and $f_w = 2V_0\sqrt{\frac{x}{v_\infty U_\infty}}$ is the suction/injection parameter.

The momentum Eq. (19) and energy Eq. (20) to have a similarity solution, the magnetic field parameter M, surface convection parameter ζ, slip parameter δ and the suction/injection parameter f_w must be a constant. Therefore, if we assume the applied magnetic field $B(x)$, convective heat transfer coefficient h_w, thermal property of liquid β' and transpiration velocity V_0 are proportional to $x^{-1/2}$ (see Ref. Alam et al. [13], Aziz [21] and Helmy [34]), then M, ζ, β and f_w will be independent of x. We therefore assume that $B(x) = B_0x^{-1/2}$, $h_w = c_1x^{-1/2}$, $\beta' = c_2x^{-1/2}$ and $V_0 = c_3x^{-1/2}$ where B_0, c_1, c_2 and c_3 are constants.

For liquid flows the slip parameter δ can be written as

$$\delta = Kn_{x,L}Re_x^{1/2} \tag{23}$$

where the local Knudsen number, $Kn_{x,L}$ based on slip length L and local Reynolds number Re_x are defined as

$$Kn_{x,L} = \frac{L}{x}, \tag{24}$$

$$Re_x = \frac{U_\infty x}{v_\infty} \tag{25}$$

It should be noted that as slip parameter δ is a function of x so for liquid flow with slip over flat plate does not possess self-similar solutions. However, since the approach preserves the mass and momentum conservation, it is still valid for the flow dynamics within the boundary layer (see Ref. Fang and Lee [17], Fang et al. [18]). So for fixed values of δ the solution of (19) subject to the boundary conditions (22) would be locally similar. Thus locally similarity approach implied that the non-dimensional quantity δ is determined for any values of x and the upstream history of the flow will be ignored, except as far as it influences the similarity variable.

Because both viscosity and thermal conductivity vary across the boundary layer, the Prandtl number also varies. Following Rahman [27], the Prandtl number is defined as

$$Pr = \frac{\mu c_p}{\kappa} = \frac{\left(\frac{\theta_r}{\theta_r-\theta}\right)\mu_\infty c_p}{\kappa_\infty(1+\epsilon\theta)} = \frac{1}{(1-\frac{\theta}{\theta_r})(1+\epsilon\theta)}Pr_\infty \tag{26}$$

With the use of (28), the non-dimensional energy Eq. (20) can be expressed as

$$(1+\epsilon\theta+Nr)\theta'' + \alpha\theta'^2 + Pr\left(1-\frac{\theta}{\theta_r}\right)(1+\alpha\theta)(f\theta' - f'\theta)$$
$$+ Q\theta + Q^* e^{-\beta\eta} = 0 \tag{27}$$

The quantities of main physical interest of the present study are the Nusselt number (rate of heat transfer) and the Sherwood number (rate of mass transfer). The equation defining the rate of heat transfer q_w, is given by

$$q_w = -\kappa\left(\frac{\partial T}{\partial y}\right)_{y=0} - \frac{4\sigma^*}{3k^*}\left(\frac{\partial T^4}{\partial y}\right)_{y=0} \tag{28}$$

Thus the rate of heat transfer in terms of the dimensionless Nusselt number is defined as follows:

$$Nu = -\frac{1}{2}Re_x^{1/2}(1+\epsilon\theta(0)+Nr)\theta'(0) \tag{29}$$

or,

$$Nu^* = -(1+\epsilon\theta(0)+Nr)\theta'(0) where Nu^* = 2Re_x^{-1/2}Nu \tag{30}$$

Similarly, the rate of mass transfer in terms of local Sherwood number is given by

$$Sh^* = -\phi'(0) \tag{31}$$

3. Method of solution

The set of Eqs. (19), (21) and (29) is highly non-linear and coupled and therefore the system cannot be solved analytically. Therefore they are solved in the symbolic computation software MATHEMATICA using shooting technique. It would be impractical to solve the system for even a very large finite interval. So, effort has been made to solve a sequence of problems posed on increasingly larger intervals to verify the solution's consistent behavior as the boundary approaches to ∞. The plot of each successive solution has been superimposed over those of previous solutions so that they can easily be compared for consistency. For numerical computation infinity condition has been taken at a large but finite value of η where no considerable variation in temperature, concentration, etc. occurs.

3.1. Testing of the code

In the absence of mass transfer, the results obtained in this work are more generalized form of Rahman [27] and so can be taken as a limiting case by taking $Nr \to 0$, Q, $Q^* \to 0$. Also the present results are in excellent agreement with the results of Das [30] in the absence of mass transfer. To check the validity of the present code, the values of $-\theta'(0)$ have been calculated for $\theta_r \to \infty$ and for different values of the surface convection parameter ζ and Prandtl number Pr using MATHEMATICA in Table 1. The result obtained herein is in good agreement with those of Rahman [27] and Das [30] for $\theta_r \to \infty$, $\epsilon = 0$, $M = 0$, $Nr = 0$, $Q = Q^* = 0$, $\tau = 0$ and $\delta = 0$, which shows the validity of the present solution and justifies the use of the present numerical code.

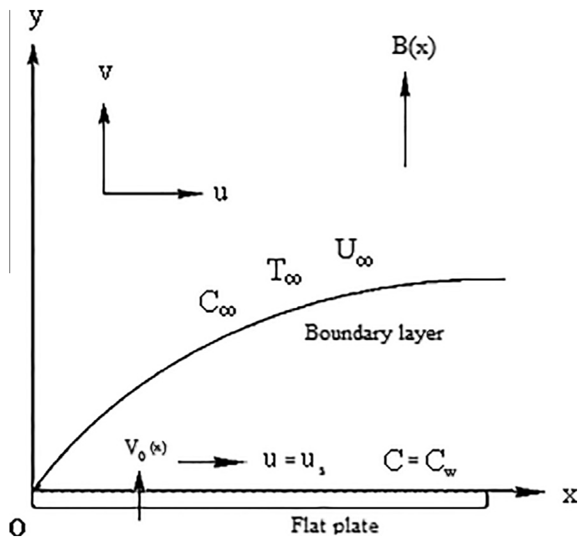

Fig. 1 Flow configuration and coordinate system.

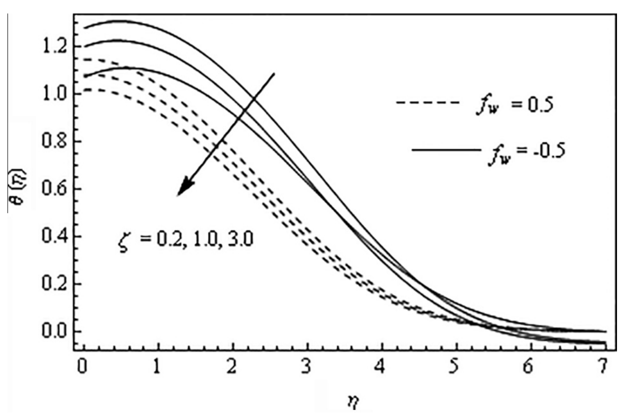

Fig. 2 Effect of surface convection parameter ζ on temperature profiles.

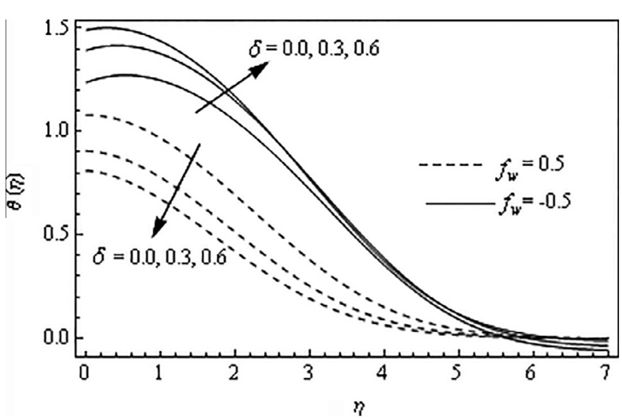

Fig. 3 Effect of slip parameter δ on temperature profiles.

4. Numerical results and discussions

In order to gain physical insight of the problem, the numerical results for temperature and concentration have been presented

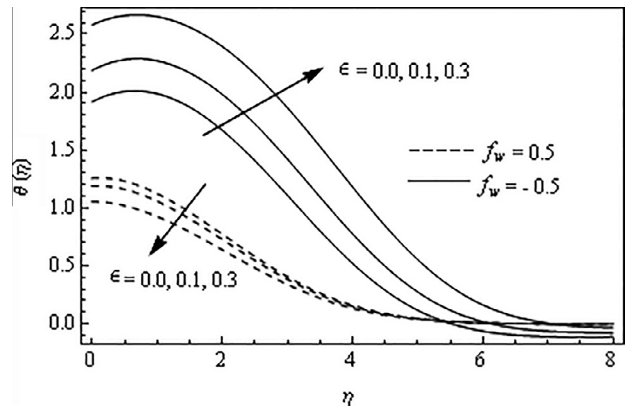

Fig. 4 Effect of thermal conductivity parameter ϵ on temperature profiles.

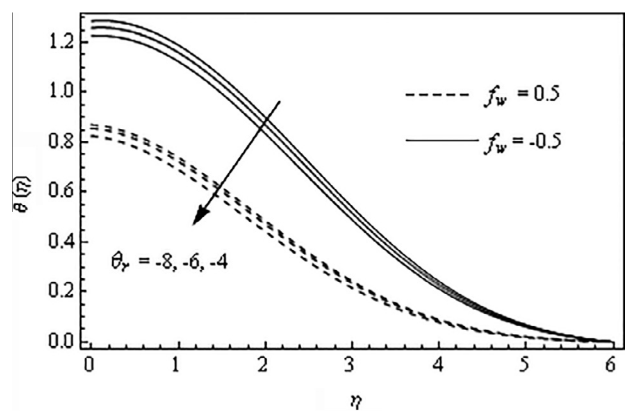

Fig. 5 Effect of viscosity parameter $\theta_r(< 0)$ on temperature profiles.

graphically in Figs. 2–13 and in Tables 1–3 for several sets of values of the pertinent parameters such as slip parameter δ, surface convection parameter ζ, variable viscosity parameter θ_r, thermal conductivity parameter ϵ, Schmidt number Sc, magnetic field parameter M, thermophoretic parameter $\tau$and suction/injection parameter f_w. It should be noted here that positive values of f_w indicate liquid suction at surface while negative values of f_w correspond to liquid blowing/injection at the wall. In the simulation the default values of the parameters are considered as $\delta = 0.1$, $\zeta = 0.2$, $\theta_r = -2.5$, $\epsilon = 0.1$, $M = 0.5$, $Nr = 0.2$, $Pr = 0.71$, $Q = 0.2$, $Q^* = 0.3$, $Sc = 0.6$, $f_w = \pm 0.5$ and $\tau = 0.2$ unless otherwise specified.

Fig. 2 demonstrates the effects of surface convection parameter ζon liquid temperature in the boundary layer region in the presence of suction as well as injection. It is observed from the figure that temperature $\theta(\eta)$ decreases on increasing ζ in the boundary layer region and is maximum at the surface of the plate in both the cases of suction and injection. Thus the thermal boundary layer thickness decreases with the increase of ζ. The solution approaches to the solution for constant surface temperature for large values of ζ i.e. $\zeta \to \infty$. From the boundary condition (22), it can be seen that $\theta(0) = 1$ as $\zeta \to \infty$. These results support the numerical results obtained in the present problem. It is worth mentioning that the parameter ζ is more influential in the case of injection in contrast with

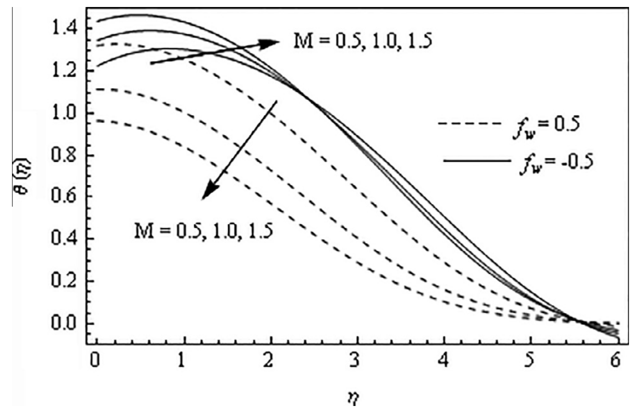

Fig. 6 Effect of magnetic field parameter M on temperature profiles.

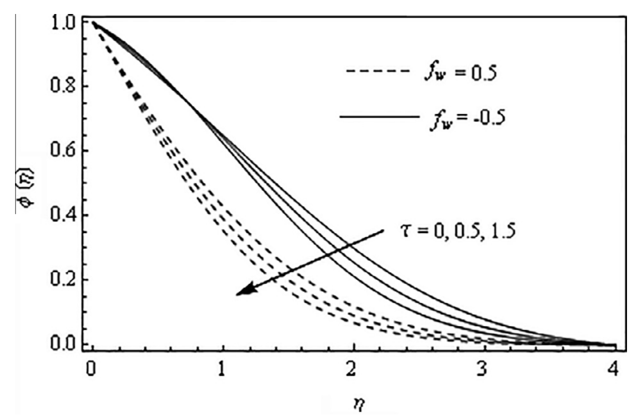

Fig. 7 Effect of thermophoretic parameter τ on concentration profiles.

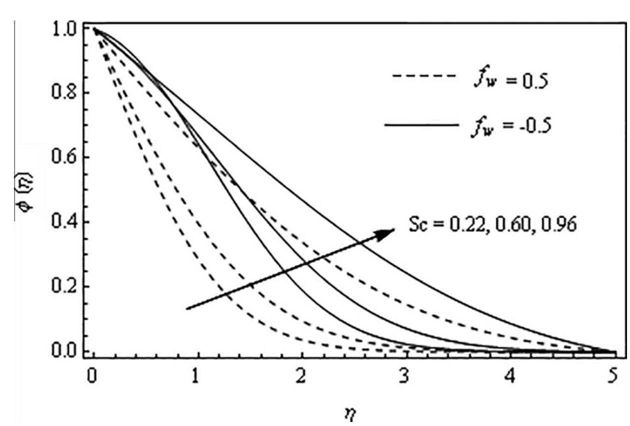

Fig. 8 Effect of Schmidt number Sc on concentration profiles.

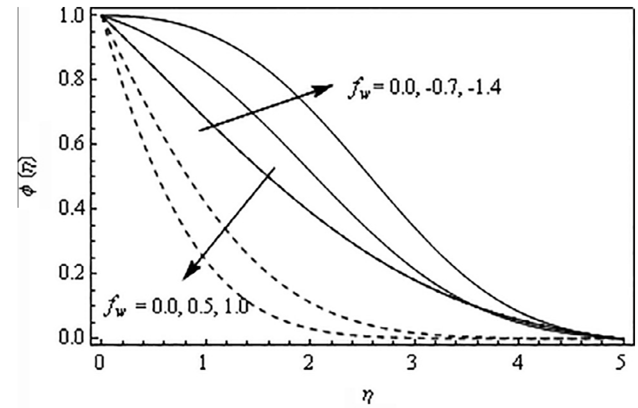

Fig. 9 Effect of suction/injection parameter f_w on concentration profiles.

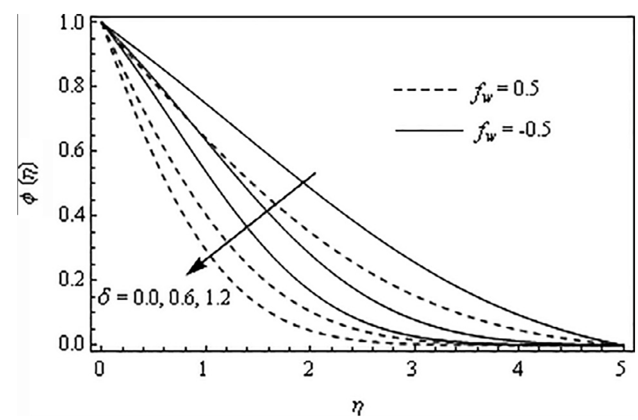

Fig. 10 Effect of slip parameter δ on concentration profiles.

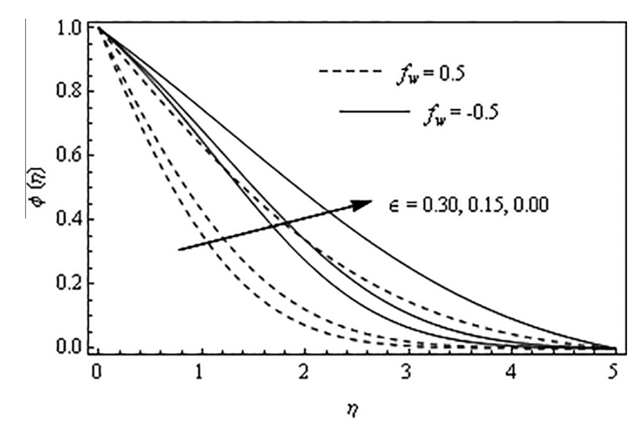

Fig. 11 Effect of thermal conductivity parameter ϵ on concentration profiles.

suction. These results are in good agreement with the results obtained by Rahman [27] and Das [30] in the absence of suction/injection.

Fig. 3 shows that the liquid temperature is the maximum near the boundary layer region and it decreases on increasing boundary layer coordinate η to approach free stream value for both suction ($f_w = 0.5$) and injection ($f_w = -0.5$). Also it is observed that the liquid temperature decreases on increasing slip parameter δ in the boundary layer region in case of suction and, as a consequence, thickness of the thermal boundary layer decreases. But the effect is opposite for injection. Further, it is evident that the effect of slip parameter δ when $f_w = -0.5$ seems to be more pronouncing compared to $f_w = 0.5$ in increasing the thermal boundary layer thickness.

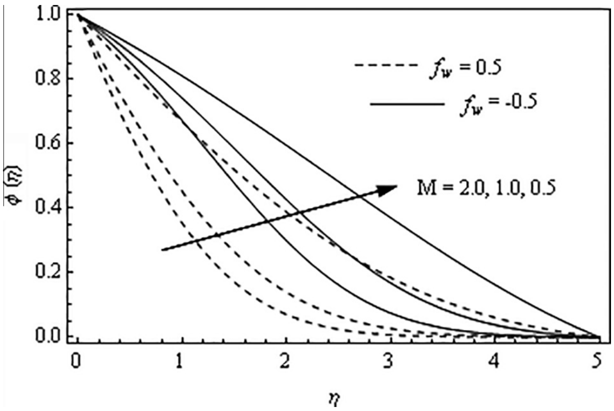

Fig. 12 Effect of magnetic field parameter M on concentration profiles.

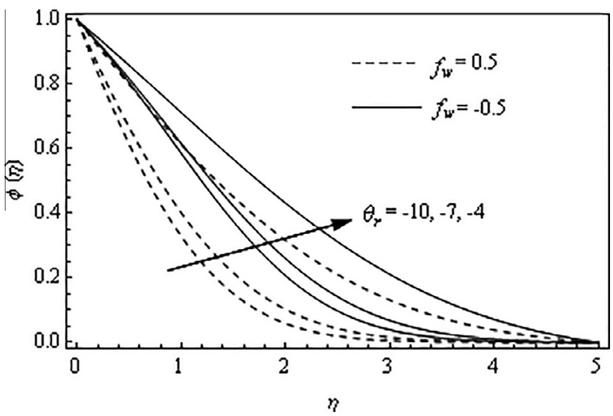

Fig. 13 Effect of viscosity parameter $\theta_r (< 0)$ on concentration profiles.

The effect of thermal conductivity parameter ϵ on temperature distribution is shown in Fig. 4 for both suction and injection. The effect of increasing ϵ from zero (constant thermal conductivity of fluid) to 0.3 induces a significant drop in the temperature in the flow domain when suction parameter $f_w = 0.5$ and hence there would be a decrease in the thermal boundary layer thickness. The influence of conductivity parameter ϵ on temperature distribution is totally opposite when injection parameter $f_w = -0.5$. But the combined effect of thermal conductivity parameter and injection on temperature distribution is prominent from the figure. Liquid temperature is therefore maximized with larger values of ϵ in the case of injection. All profiles decay smoothly from maximum values at the wall to zero in the free stream (edge of the boundary layer).

The influence of viscosity parameter θ_r on temperature distribution is highlighted in Fig. 5. It is seen that temperature profiles rise with the increase of absolute value of θ_r when θ_r is negative in the presence of suction as well as injection and hence, there would be an increase in the thermal boundary layer thickness. The figures also project that the thermal boundary layer thickness is more in the case of injection than in the case of suction. These observations show good agreement with the results obtained by Rahman [27] in the absence of suction/injection.

Table 2 Effects of f_w, ζ, τ, δ and M on Nu^* and Sh^*.

f_w	ζ	τ	δ	M	Nu^*	Sh^*
0.5	0.2	0.2	0.3	1.5	0.019437	0.676632
	1.0				0.0321745	–
	5.0				0.0367981	–
	∞				0.0380042	–
		0.0			–	0.680311
		0.5			–	0.671308
		1.5			–	0.655187
			0.0		0.0041192	0.636595
			0.3		0.0244911	0.691135
			0.6		0.0343815	0.721639
				0.0	−0.107752	0.532037
				1.0	0.0184369	0.683917
				2.0	0.0426934	0.745586
−0.5	0.2	0.2	0.3	1.5	−0.224361	0.234927
	1.0				−0.188535	–
	5.0				−0.187507	–
	∞				−0.187794	–
		0.0			–	0.254436
		0.5			–	0.205852
		1.5			–	0.110766
			0.0		−0.299324	0.0256501
			0.3		−0.256058	0.0747253
			0.6		−0.224361	0.110766
				0.0	−0.478520	0.0741549
				1.0	−0.256058	0.210459
				2.0	−0.126539	0.342004

Table 1 Comparison of the values of $-\theta'(0)$ for various values of ζ in the absence of mass transfer.

ζ	Rahman [27]		Das [30]		Present results	
	$Pr = 0.1$	$Pr = 0.71$	$Pr = 0.1$	$Pr = 0.71$	$Pr = 0.1$	$Pr = 0.71$
0.05	0.036900	0.042781	0.036866	0.042767	0.036863	0.042762
0.1	0.058423	0.074757	0.058393	0.074724	0.058371	0.074762
0.2	0.082477	0.119358	0.082473	0.119295	0.082483	0.119288
0.4	0.103865	0.170089	0.103894	0.169994	0.103876	0.169952
0.6	0.113688	0.198155	0.113741	0.198051	0.113722	0.198051
0.8	0.119329	0.215976	0.119400	0.215864	0.119400	0.215865
1.0	0.122999	0.228303	0.123074	0.228178	0.123039	0.228178
5.0	0.136400	0.279283	0.136515	0.279131	0.136519	0.279135
10.0	0.138279	0.287291	0.138404	0.287146	0.138404	0.287146

Table 3 Effects of f_w, θ_r, ϵ and Sc on Nu^* and Sh^*.

f_w	θ_r	ϵ	Sc	Nu^*	Sh^*
0.5	1.0	0.15	0.60	−0.0771143	0.642955
	3.0			0.0106725	0.697304
	∞			0.0425222	0.720749
	−2.0			0.0695976	0.740066
	−4.0			0.0604331	0.733101
	−8.0			0.0526748	0.728838
	2.0	0.0		0.0904339	.600936
		0.1		−0.0571169	0.655241
		0.3		−0.0058659	0.675667
			0.22	–	0.372136
			0.60	–	0.683917
			0.96	–	0.958001
−0.5	1.0	0.15	0.60	−0.196341	0.272848
	3.0			−0.296854	0.242964
	∞			−0.106367	0.317641
	−2.0			−0.0392842	0.345051
	−4.0			−0.060858	0.337433
	−8.0			−0.073999	0.332456
	2.0	0.0		0.0129973	−0.0711031
		0.1		−0.256761	0.261862
		0.3		−0.25531	0.246459
			0.22	–	0.207304
			0.60	–	0.234927
			0.96	–	0.257302

The impact of magnetic field parameter M on the temperature profiles is presented in Fig. 6 for both suction and injection. It can easily be seen from the figure that the temperature decreases as the boundary layer coordinate η increases for a fixed value of M. For a non-zero fixed value of η, temperature distribution across the boundary layer decreases with the increasing values of M for suction and hence the thickness of thermal boundary layer decreases. But in case of injection, liquid temperature increases with the increase in the magnetic field parameter M at all points of the flow field near the boundary surface, i.e., for $\eta < 2.5$ (not precisely determined) whereas, the reverse effect occurs for $\eta > 2.5$ (not precisely determined). For both suction and injection, surface temperature of the plate can be controlled by controlling the strength of the applied magnetic field.

Fig. 7 illustrates the variation of the concentration distribution across the boundary layer for various values of the thermophoretic parameter τ for both suction and injection. It is seen that the effect of increasing values of the thermophoretic parameter results in decreasing concentration distribution across the boundary layer. This is true in both suction as well as injection, but the concentration distribution is weakly dependent on the thermophoresis for $\eta < 1$ (not precisely determined) in the case of injection. It is worth mentioning that the concentration boundary layer thickness is more in the case of injection than in the case of suction.

Fig. 8 draws out the effect of the Schmidt number Sc on the variation of concentration profiles for the suction case $f_w = 0.5$ as well as for the injection case $f_w = -0.5$. Species diffusion (concentration) is found to increase with an increase in Sc, i.e., it is maximized for the highest value of Sc. This is true in both suction as well as injection. Therefore, concentration boundary layer thickness will also be maximized by the highest value of Sc in the case of suction and injection. All profiles descend monotonically from one at the wall to zero in the free stream.

It is observed from Fig. 9 that the concentration profiles decrease with increasing suction parameter f_w but the effect is opposite for injection. Also the concentration boundary layer thickness is more in the case of injection than in the case of suction. Fig. 10 depicts chemical species concentration profiles against η for various values of slip parameter δ. It is seen that concentration of the liquid decreases dramatically with an increase of the slip parameter throughout the domain (i.e. $0 < \eta < 1$) for both the cases of suction and injection. But the effect is prominent for suction. Increasing slip parameter adds to the velocity slip on the wall. As a result, it decreases the concentration in the boundary layer region.

Fig. 11 shows the influence of thermal conductivity parameter ϵ on the dimensionless concentration function ϕ. An increase in ϵ causes a distinct fall in the concentration profiles for both suction ($f_w = 0.5$) and injection ($f_w = -0.5$). The case $\epsilon = 0$ corresponds to the constant conductivity of the fluid. It is also found that concentration distribution in the boundary layer region is higher for the case of a constant conductivity than for the variable conductivity, which is true for both cases of $f_w > 0$ and $f_w < 0$. All profiles decay to the free stream value of zero as $\eta \to \infty$. It is worthy to be noted that thermal conductivity parameter has a pronounced effect on species concentration for $f_w > 0$.

The variation of concentration profiles for different values of magnetic field parameter M for both suction and injection at the boundary are presented in Fig. 12. It is noticeable that concentration profiles within the boundary layer decreases with an increase of applied magnetic field. This behavior is due to the growing effect of the Lorentz force in the flow regime.

In Fig. 13, we have studied the detail effects of $\theta_r < 0$ on the concentration fields considering suction and injection. For $\theta_r < 0$ concentration boundary layer thickness decreases with the increase of $|\theta_r|$ for both the cases of suction and injection. But it is worth mentioning that the distribution of concentration is more effective in the case of injection than in the case of suction. The decrease in thickness of the concentration layer is caused by the dual effects; (i) the direct action of suction/injection, and (ii) the indirect action of suction/injection causing a thicker thermal boundary layer, which corresponds to lower temperature gradient, a consequent increase in the thermophoretic force and higher concentration gradient.

The influence of the surface convection parameter ζ, slip parameter δ, magnetic field parameter M, thermophoretic parameter τ, variable viscosity parameter θ_r, thermal conductivity parameter ϵ, Schmidt number Sc in the presence of suction and injection on the dimensionless Nusselt number Nu^* and Sherwood number Sh^* can be seen in Tables 2 and 3. From the table it is observed that Nu^* increases with increasing ζ when $f_w = 0.5$ but the effect is opposite $f_w = -0.5$. As thermophoretic parameter τ increases, rate of mass transfer decreases for both the cases of suction and injection. It is evident from the tables that the slip parameter enhances both the Nusselt number and the Sherwood number for suction ($f_w = 0.5$) as well as injection ($f_w = -0.5$). This phenomenon is true even in the presence of thermal radiation and non-uniform heat source/sink. It is interesting to note that the rate of heat and mass transfer increases with the increase in the strength of applied magnetic field in the presence of suction/injection. One may note that the value of Nu^* is negative for some values of material parameters. This means heat flows from the liquid to the flat surface. The Schmidt number Sc tends to raise the Sherwood number by increasing concentration gradient on the wall. The reason for this trend is that the concentration boundary layer becomes thin for large Schmidt numbers. As thermal conductivity parameter ϵ increases, both Nusselt number and Sherwood number get reduced for both suction ($f_w = 0.5$) and injection ($f_w = -0.5$). The impact of variable viscosity parameter θ_r on Nu^* and Sh^* is presented in Table 3. It is observed from this table that variable viscosity parameter enhances the dimensionless Nusselt number and Sherwood number for suction ($f_w = 0.5$) whereas the effect is fluctuating in nature for injection ($f_w = -0.5$). From Tables 2 and 3, it is perceived that the rate of mass transfer is more in the case of suction than in the case of injection, whereas the reverse effect occurs for the rate of heat transfer.

5. Conclusions

This paper studies the effects of thermophoretic particle deposition on steady two dimensional MHD boundary layer flow of an incompressible electrically conducting liquid over a permeable flat plate with partial slip at the surface of the boundary and convective surface heat flux in the presence of suction or injection with variable liquid properties. Following conclusion can be drawn from the present investigation:

- The influences of thermophoresis, slip velocity and variable liquid properties can act simultaneously and their interactions must be considered for the accurate prediction of heat and mass transfer rate and other effects.
- The thermal boundary layer for injection is more dominant in comparison with that for suction.
- Temperature in the boundary layer is strongly increased with slip parameter, variable viscosity parameter, magnetic field parameter and thermal conductivity parameter in the case of suction while the opposite effect is observed in the case of injection.
- Thermal boundary layer thickness reduces with increase of surface convection parameter for both suction as well as injection.
- The species concentration decreases with increase of thermophoretic parameter, slip parameter, thermal conductivity parameter, variable viscosity parameter and suction parameter but reverse behavior occurs for Schmidt number and injection parameter.
- Thermophoretic particle deposition increases the rate of mass transfer on the wall.
- The impact of suction/injection on the boundary layer growth is significant due to the decrease in the thickness of the thermal and concentration boundary layer.

Acknowledgments

The authors wish to express their sincere thanks to the honorable referees for the valuable comments and suggestions to improve the quality of the paper.

References

[1] P. Goldsmith, F.G. May, Diffusiophoresis and thermophoresis in water vapour systems, in: C.N. Davies (Ed.), Aerosol, Science, Academic Press, London, 1966, pp. 163–194.

[2] S.L. Goren, Thermophoresis of aerosol particles in laminar boundary layer on flat plate, J. Colloid Interface Sci. 61 (1977) 77–85.

[3] L. Talbot, R.K. Cheng, R.W. Schefer, D.R. Willis, Thermophoresis of particles in a heated boundary layer, J. Fluid Mech. 101 (1980) 737–758.

[4] G.K. Batchelor, C. Shen, Thermophoretic deposition of particles in gas flowing over cold surfaces, J. Colloid Interface Sci. 107 (1985) 21–37.

[5] S. Jayaraj, K.K. Dinesh, K.L. Pallai, Thermophoresis in natural convection with variable properties, Heat Mass Transfer 34 (1999) 469–475.

[6] A. Selim, M.A. Hossain, D.A.S. Rees, The effect of surface mass transfer on mixed convection flow past a heated vertical flat permeable plate with thermophoresis, Int. J. Therm. Sci. 42 (1999) 973–982.

[7] A.J. Chamkha, I. Pop, Effects of thermophoresis particle deposition in free convection boundary layer from a vertical flat plate embedded in a porous medium, Int. Commun. Heat Mass Transfer 31 (2004) 421–430.

[8] A.J. Chamkha, A.F. Al-mudhaf, I. Pop, Effects of heat generation or absorption on thermophoretic free convection boundary layer from a vertical flat plate embedded in a porous medium, Int. Commun. Heat Mass Transfer 33 (2006) 1096–1102.

[9] M.K. Partha, Suction/injection effects on thermophoresis particle deposition in a non-Darcy porous medium under the influence of Soret, Dufour effects, Int. J. Heat Mass Transfer 52 (2009) 1971–1979.

[10] A.Y. Bakier, R.S.R. Gorla, Effects of thermophoresis and radiation on laminar flow along a semi-infinite vertical plate, Heat Mass Transfer 47 (4) (2011) 419–425.

[11] A. Postelnicu, Thermophoresis particle deposition in natural convection over inclined surfaces in porous media, Int. J. Heat Mass Transfer 55 (2012) 2087–2094.

[12] N.K. Varshney, S. Kumar, Magneto-hydrodynamics boundary layer flows of non-Newtonian fluid past a flat plate through a porous medium, Bull. Calcutta Math. Soc. 97 (2005) 21–30.

[13] M.S. Alam, M.M. Rahman, M.A. Sattar, On the effectiveness of viscous dissipation and Joule heating on steady magnetohydrodynamic heat and mass transfer flow over an inclined radiate isothermal permeable surface in the presence of thermophoresis, Commun. Nonlinear Sci. Numer. Simul. 14 (2009) 2132–2143.

[14] A.J. Chamkha, I. Camille, Effects of heat generation/absorption and thermophoresis on hydromagnetic flow with heat and mass transfer over a flat surface, Int. J. Numer. Methods Heat Fluid Flow. 10 (2000) 432–448.

[15] J. Zueco, O.A. Bég, H.S. Takhar, V.R. Prasad, Thermophoretic hydromagnetic dissipative heat and mass transfer with lateral mass flux, heat source, Ohmic heating and thermal conductivity effects: Network simulation numerical study, Appl. Thermal Eng. 29 (2009) 2808–2815.

[16] N.F.M. Noor, S. Abbasbandy, I. Hashim, Heat and mass transfer of thermophoretic MHD flow over an inclined radiate isothermal permeable surface in the presence of heat source/sink, Int. J. Heat Mass Transfer 55 (2012) 2122–2128.

[17] T. Fang, C.F. Lee, Exact solutions of incompressible Couette flow with porous walls for slightly rarefied gases, Heat Mass Transfer 42 (2006) 255–262.

[18] T. Fang, J. Zhang, S. Yao, Slip MHD viscous flow over a stretching sheet – an exact solution, Commun. Nonlinear Sci. Numer. Simul. 14 (2009) 3731–3737.

[19] C.Y. Wang, Analysis of viscous flow due to a stretching sheet with surface slip and suction, Nonlinear Anal. Real World Appl. 10 (2009) 375–380.

[20] T. Fang, S. Yao, J. Zhang, A. Aziz, Viscous flow over a shrinking sheet with a second order slip flow model, Commun. Nonlinear Sci. Numer. Simul. 15 (2010) 1831–1842.

[21] A. Aziz, Hydrodynamic and thermal slip flow boundary layers over a flat plate with constant heat flux boundary condition, Commun. Nonlinear Sci. Numer. Simul. 15 (2010) 573–580.

[22] K. Das, Slip effects on heat and mass transfer in MHD micropolar fluid flow over an inclined plate with thermal radiation and chemcal reaction, Int. J. Numer. Meth. Fluids 70 (2012) 96–113.

[23] T.C. Chiam, Heat transfer in a fluid with variable thermal conductivity over a linearly stretching sheet, Acta Mech. 129 (1998) 63–72.

[24] M.M. Rahman, M.J. Uddin, A. Aziz, Effects of variable electric conductivity and non-uniform heat source (or sink) on convective micropolar fluid flow along an inclined flat plate with surface, Int. J. Therm. Sci. 48 (2009) 2331–2340.

[25] R. Kandasamy, I. Muhaimin, A.B. Khamis, Thermophoresis and variable viscosity effects on MHD mixed convective heat and mass transfer past a porous wedge in the presence of chemical reaction, Heat Mass Transfer 45 (2009) 703–712.

[26] K.V. Prasad, K. Vajravelu, P.S. Datti, The effects of variable fluid properties on the hydro-magnetic flow and heat transfer over a non-linear stretching sheet, Int. J. Therm. Sci. 49 (2010) 603–610.

[27] M.M. Rahman, Locally similar solutions for hydromagnetic and thermal slip flow boundary layers over a flat plate with variable fluid properties and convective surface boundary condition, Meccanica 46 (5) (2011) 1127–1143.

[28] M.M. Rahman, A. Aziz, M. AI-Lawatia, Heat transfer in micropolar fluid along an inclined permeable plate with variable properties, Int. J. Therm. Sci. 49 (2010) 993–1002.

[29] J. Zueco, O.A. Beg, L.M. Lopez-Ochoa, Effects of thermophoresis particle deposition and of the thermal conductivity in a porous plate with dissipative heat and mass transfer, Acta Mech. Sinica 27 (2011) 383–398.

[30] K. Das, Impact of thermal radiation on MHD slip flow over a flate plate with variable fluid properties, Heat Mass Transfer 48 (2012) 767–778.

[31] J.X. Ling, A. Dybbs, Forced convection over a flat plate submersed in a porous medium: variable viscosity case, ASME, Paper 87-WA/HT-23, ASME Winter Annual Meeting, Boston, Massachusetts, 1987, pp. 13–18.

[32] E.M. Abo-Eldahab, M.A. EI-Aziz, Blowing/suction on hydromagnetic heat transfer by mixed convection from an inclined contonuously stretching surface with internal heat generation/absorption, Int. J. Therm. Sci. 43 (2004) 709–719.

[33] T.A. Savvas, N.C. Markatos, C.D. Papaspyrides, On the flow of non-Newtonian polymer solutions, Appl. Math. Model. 18 (1994) 14–22.

[34] K.A. Helmy, MHD boundary layer equations for power law fluids with variable electric conductivity, Meccanica 30 (1995) 187–200.